10-2-2020

New transitions and levels for Tb 163 obtained from β -decay studies

C. J. Zachary
Vanderbilt University

E. Wang
Vanderbilt University

N. T. Brewer
Vanderbilt University

J. C. Batchelder
University of California, Berkeley

J. H. Hamilton
Vanderbilt University

See next page for additional authors

New transitions and levels in ^{163}Gd from β decay studies

C. J. Zachary,[1,*] N. T. Brewer,[1,2] E. Wang,[1] J. H. Hamilton,[1] J. M. Eldridge,[1] B. M. Musangu,[1] A. V. Ramayya,[1] J. K. Hwang,[1] J. C. Batchelder,[3] C. J. Gross,[2] R. Gryzwacz,[4,2] M. Madurga,[4] C. Jost,[4] D. Miller,[4] C. Bingham,[4] L. Cartegni,[4] M. Karny,[2] A. A. Fijałkowska,[4,5] S. H. Liu,[3] K. Miernik,[2,5] S. W. Padgett,[4] S. V. Paulauskas,[4] S. V. Ilyushkin,[6] J. A. Winger,[6] K. P. Rykaczewski,[2] D. W. Stracener,[2] M. Wolińska-Cichocka,[2,7] R. Surman,[8] A. C. Dai,[9] F. R. Xu,[9] Y. X. Liu,[10] and Y. Sun[11]

[1]*Department of Physics and Astronomy, Vanderbilt University Nashville, TN 37240, United States of America*
[2]*Physics Division, Oak Ridge National Laboratory, Oak Ridge, Tennessee 37931, United States of America*
[3]*UNIRIB/Oak Ridge Associated Universities, Oak Ridge, Tennessee 37831, United States of America*
[4]*University of Tennessee, Knoxville, Tennessee 37996, United States of America*
[5]*Faculty of Physics, University of Warsaw, Warsaw, PL 00-681, Poland*
[6]*Department of Physics and Astronomy, Mississippi State University, Mississippi 39762, United States of America*
[7]*Heavy Ion Laboratory, University of Warsaw, Warsaw, PL 02-093, Poland*
[8]*Department of Physics, Union College, Schenectady, New York, 12308, United States of America*
[9]*School of Physics, Peking University, Beijing 100871, People's Republic of China*
[10]*Department of Physics, Huzhou University, Huzhou 313000, People's Republic of China*
[11]*School of Physics and Astronomy, Shanghai Jiao Tong University, Shanghai 200240, People's Republic of China*

(Dated: December 5, 2019)

Background: Neutron rich nuclei in the mass region between 132 and 208 have been and will continue to be of interest for the study of nuclear structure because of the rapid onset of deformation between 88 and 90 neutrons. The observation of detailed changes in nuclear structures within this mass region has provided and will continue to provide insight into the nuclear force.

Purpose: Investigations of γ-rays emitted following ^{163}Eu β-decay to ^{163}Gd have been performed for evaluation of the nuclear structure of ^{163}Gd.

Method: Data were collected at the LeRIBSS station of the Holifield Radioactive Ion Beam Facility at Oak Ridge National Laboratory with an array of four Clover HPGe detectors for γ-rays and 2 plastic scintillators for β detection. The γ-rays were identified as belonging to ^{163}Gd via mass selection and γ-γ-β, x-ray-γ, or γ-γ coincidences.

Results: In total 107 new γ-ray transitions were observed in ^{163}Gd from 53 newly identified levels.

Conclusions: The structure of ^{163}Gd has been identified for the first time. This sturcute has been evaluated in comparison to Projected Shell Model, and Potential Energy Surface calculations with good agreement.

I. INTRODUCTION

In continuance of the study of the mass 132-208 region of rapid onset of deformation, mass $162-165$ europium isotopes were produced for β-decay studies of levels in the daughter isotopes at the Holifield Radioactive Ion Beam Facility in Oak Ridge National Lab.

Previous total absorption studies by Hayashi, *et al.* [1] have identified the Q_β for ^{163}Gd as 3170(70) keV, and its parent isotope, ^{163}Eu, Q_β as 4829(65) keV. A study with the JAEA-ISOL by Sato, *et al.* [2] identified 5 transitions with energies 85.8, 116, 138, 191.2, and 401 keV in ^{163}Gd without level assignments. All of the 5 previously observed transitions have been confirmed and 107 new transitions identified, 18 of which are tentative, between 53 new levels, three of which are tentative. The newly identified rotational band structure of ^{163}Gd is based upon systematics for N=99 low energy rotational band structure of ^{165}Dy [3–5] and projected shell model calculations. In addition many new high energy levels have been observed for ^{163}Gd.

An isomer has been observed previously in ^{163}Gd by Hayashi *et al.* with a half-life of 23.5(10)s [1]. This is of special interest in the low energy band structure of ^{163}Gd. Consistent with Hayashi *et al.*'s [1] observation, this work assigns the ground state as the $7/2^+[633]$ with the $1/2^-[521]$ being the low energy isomeric state observed by Hayashi *et al.* [1]. Such an assignment would result in an isomeric transition between the $1/2^-[521]$ and $7/2^+[633]$ levels. Projected shell model calculations included in this work confirm this relationship with good agreement between proposed levels and calculated excitations.

The elevation of the $1/2^-[521]$ above the $7/2^+[633]$ for N=99 would provide further evidence for the subshell gap begining at N=98, as discussed in the study of nearby mass ^{162}Gd by Hartley *et al.* [6]. A description further supported by the observed excitation energy of the $5/2^-[523]$ 1-qp state.

II. EXPERIMENTAL METHODS

For this study a 10-18 μA beam of 50 MeV protons was used to induce fission in a UCx target on a High

* christopher.j.zachary@vanderbilt.edu

Voltage platform to produce $^{162-165}$Eu via fission at the Holifield Radioactive Ion Beam Facility at Oak Ridge National Lab. After fission, ions were accelerated off the HV platform and passed through a high-resolution isobar separator that provided an isotopically pure beam to LeRIBSS. The beam was implanted onto a movable tape. After a designated measurement time, the moving tape controller (MTC) would transport the accumulated source behind a shield to prevent additional background from undesired daughter products, then a new source would be collected. This is referred to here as the tape cycle. The MTC settings for source collection time and measurement time were selected to best allow for observation of wanted products as selected from previously measured half-lives of europium and gadolinium isotopes. These settings were for a 30 second collection time and a 25 second decay time. For ^{163}Eu the half-life was measured by Osa, *et al* [7] to be 7.7(4)s and by Sato, et al. [2] to be 7.8(5)s. The half-life of ^{163}Gd was measured as 68(3)s by Gehrke *et al.* [8].

The detector array used was a Clover Array for Radioactive Decay Spectroscopy (CARDS) of four HPGe clover detectors, for the detection of γ-rays, operated without Compton suppression, oriented around the beam line. The four Clover detectors were located on a single plane normal to the beamline with 90° angles between each adjacent Clover. Adjacent the HPGe clovers were two plastic scintillators for β-ray detection. The scintillators allowed for gating on β signals with coincident γ-ray signals without obtaining β spectroscopy. Data acquisition was via digital pulse processing with Pixie16 modules according to methods detailed by Grzywacz [9]. This array allowed for coincident analysis with γ-γ, x-ray-γ, γ-tape cycle, γ-β-tape cycle and associated projections.

III. RESULTS

The 5 previously identified transitions have been observed in this work to be 85.3, 115.9, 137.8, 191.7, and 400.9 keV. These previously identified transitions and the characteristic x-rays for ^{163}Gd were used to confirm transitions associated with the de-excitation of ^{163}Gd via $\gamma-\gamma$, x-ray-γ, $\beta-\gamma$, and $\gamma-$Tape-cycle coincidences. Additionally 107 new transitions have been identified, 18 of which are tentative, between 53 new levels, 3 of which are tentative. The full decay scheme obtained in this work is shown in Figures 1 and 2.

Figure 3 (j) and (k) show spectra of those γ-transitions coincident with the 85.3 keV transition. Therein are clearly observed the 104.5, 440.8, 446.4, 486.9, 952.1, 974.8, 992.4, 1015.1, 1427.4, and 1713.2 keV transitions. Gates on each of these transitions are consistent with their assignments. The gate on the 104.5 keV γ-ray, not shown, allows observation of the 651.0 keV transition, which is of low intensity and is not distinguishable from the background in the coincidence spectra of the strong 85.3 keV transition. Also seen in the 85.3 keV coincidence spectra are evidences for a number of transitions that are not observed in gates for any other transitions but whose coincidence spectra are consistent with their assignment: 607.7, 671.7, 2177.4, 2235.2, 2247.0, 2310.9, (2431.0), (2490.1), and (2576.4) keV transitions. Furthermore the 2317.6 and 2325.3 keV transitions are contributing to this spectra though not well resolved from the 2310.9 keV peak in this frame.

Seen in Figure 3 (h) and (i) are transitions coincident with the 191.7 keV transition; (53.1), 71.8, 74.8, 96.2, (130.4), 170.9, 1002.1, 1834.7, 1859.1, 1909.8, 2030.2, and 2126.5 keV. The (53.1) keV transition in this gate is weakly observed on the shoulder of the 50 keV x-ray peak and would correspond to feeding from the 454.4 keV level. However, the (53.1) keV transition is in a region of very strong internal conversion and gates upon the (53.1) keV transition do not confirm this assignment, therefore, it is only tentatively placed. The (130.4) keV transition matches the energy to originate from the 531.7 keV level to the 401.3 keV level, but a gate on (130.4) keV does not show all of the expected coincident transitions and is thus included tentatively.

In frame (f) of Figure 3 are seen transitions coincident with the 1758.2 transition. The 400.9, 516.8, and 538.7 keV transitions demonstrate clear coincidence with the 1758.2 keV transition. Similarly, frame (d) shows coincident spectra for the gate on the 1816.0 keV transition. The transitions of 459.1, 480.9, and 530.9 keV are observed without clear observation of any additional transitions.

In frame (g) of Figure 3 is seen the coincidence spectra for a gate on the 1037.4 keV transition, demonstrating coincidence with the 1225.3, 1358.8, 1402.2, 1447.2, and 1490.4 keV transitions. In frame (e) of Figure 3 is seen the coincidence spectra for a gate on the 454.4 keV transition, demonstrating coincidence with the 1002.1, 1699.6, 1799.1, 1808.3, 1856.7, 1903.6, (1985.3), and 2030.2 keV transitions.

Frames (a) and (b) are gates upon the 115.9 and 137.8 keV transitions. Evidence is seen in these separate gates for the 71.8 keV transition and the 50.0 keV transition, respectively. Note that while the 50.0 keV peak appears in both spectra, it is strongly enhanced in the 137.8 keV gate because this transition overlaps in energy the K_b x-rays for ^{163}Gd. The enhancement observed only in the 137.8 keV gate is because the 50.0 keV coincident γ-ray transition adds intensity to the x-ray peak while the peak observed in 115.9 keV gate is expected to be predominantly from the K_b x-rays from ^{163}Gd. Observed between both gates are also the 75.8, 400.9, 480.6, 583.5, and 599.3 keV transitions. The higher energy 2165.9, 2202.3, 2217.4, and 2260.2 keV transitions which feed the 325.5 keV level from higher in the structure are shown in frame (a) and are also observed in the gate upon 115.9 keV though not shown here.

Frame (c) displays the spectra obtained from a gate on 646.3 keV. Here is observed evidences for the 992.4, 1616.5, 1664.9, 1728.7, 1750.0, 1764.4, and 1838.4 keV transitions to the 646.3 keV level. The 646.3 keV level is tentatively assigned as the 3/2+ band head, along with

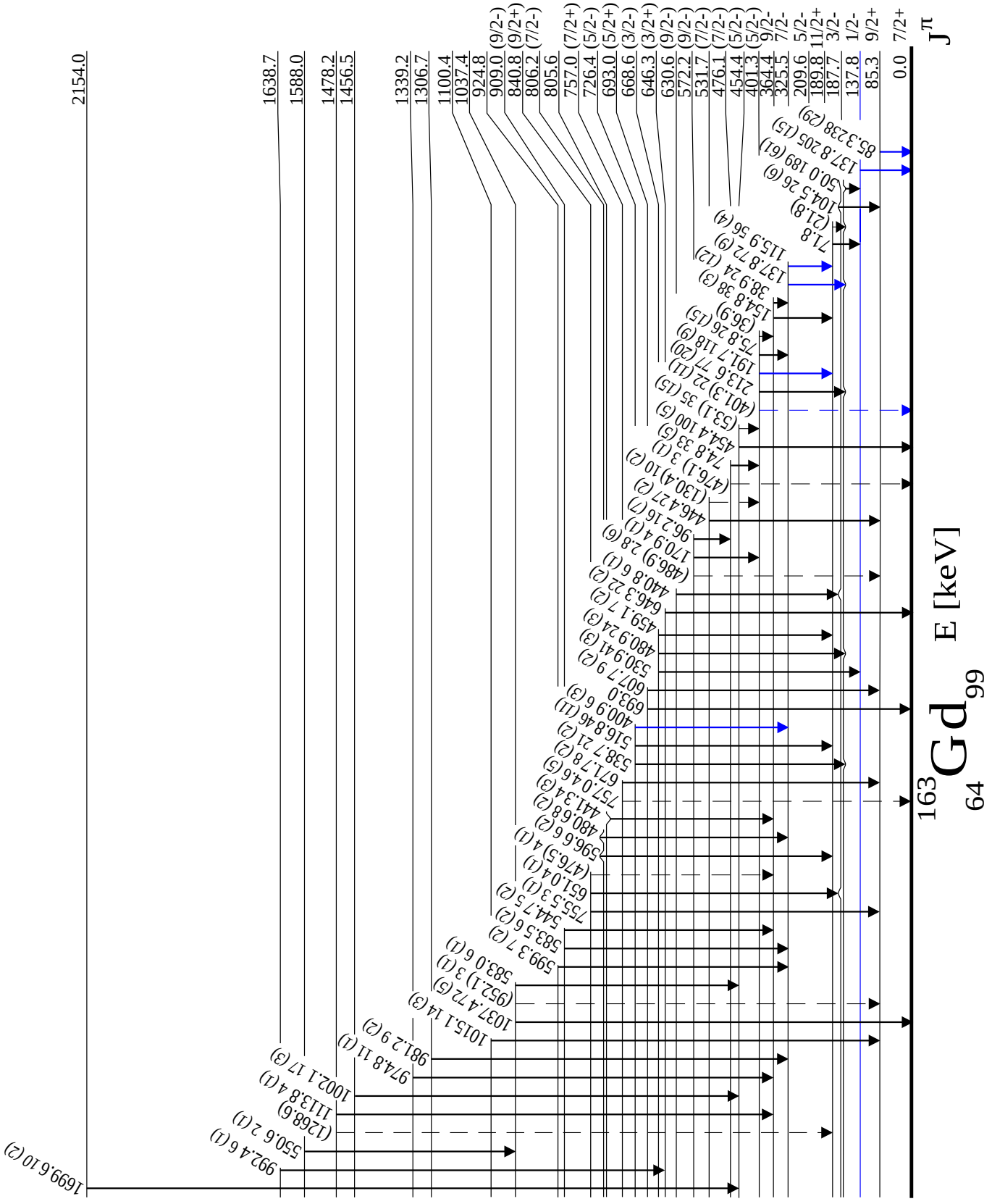

FIG. 1. Level scheme of ^{163}Gd. New transitions and levels in black, previously identified transitions in blue. $T_{1/2}$ of 137.8 keV level 23.5(10)s[1].

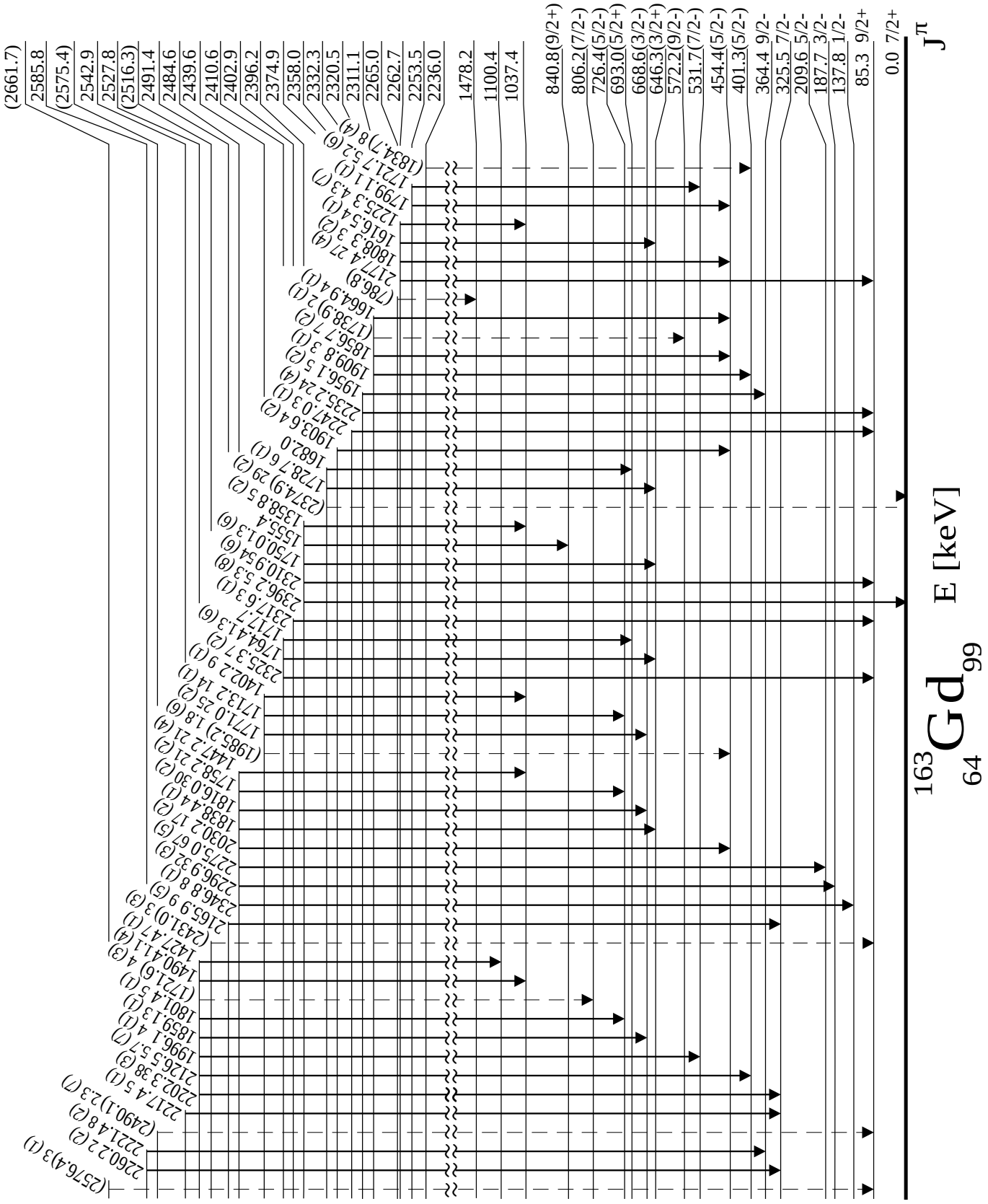

FIG. 2. Level scheme of ^{163}Gd continued. All transitions and levels are new.

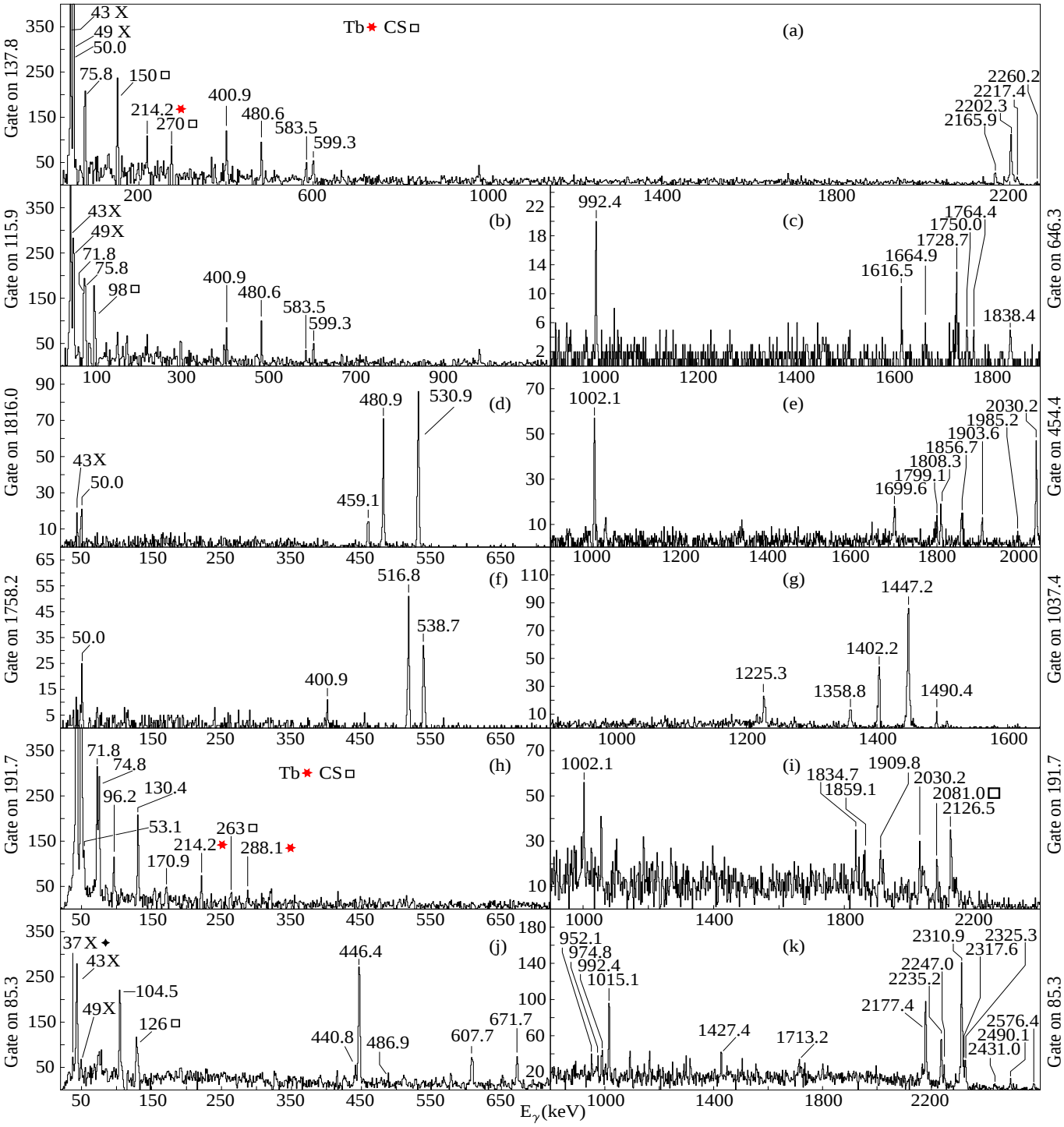

FIG. 3. Coincidence spectra for background subtracted gates on ^{163}Gd transitions; (a) 137.8 keV, (b) 115.9 keV, (c) 1816.0 keV, (d) 454.4 keV, (e) 1758.2 keV, (f) 1037.4 keV, (g)&(h) 191.7 keV, (i)&(j) 85.3 keV. Where CS indicates a Compton Scatter peak.

rotational excitations at levels 693.0, 757.0, and 840.8 keV as discussed in the following section.

As for the remaining transitions identified in ^{163}Gd at 2030.2, 2346.8, (2374.9), and 2396.2 keV, they are not clearly present in the coincidence gates shown but are coincident with appropriate K x-ray peaks, and are present in the singles spectra, not shown. The (2374.9) keV transition is listed as tentative due to a lack of any other observed transitions coincident with the (2374.9) keV transition, an alternate location for this transition would be feeding the 137.8 keV $1/2^-$ level, which is an isomer and feeding to this state would be consistent with non-observation of other coincident transitions.

Tables I, II, and III list every transition observed in

TABLE I. Transitions in ^{163}Gd. Transition energy, intensity, internal conversion corrected intensity, assumed multipolarity for ICC, energy and J^π of initial and final levels. J^π assignments from systematics with ^{165}Dy, [3–5].

E_γ keV	I_γ%	I_γ%ICC	ICC	$Multipolarity$	E_i	E_f	J_i^π	J_f^π
(21.8)(5)					209.6(7)	187.7(7)	$5/2^-$	$3/2^-$
(36.9)(5)					401.3(7)	364.4(7)	$(5/2^-)$	$9/2^-$
38.9(5)	4(2)	24(12)		M1	364.4(7)	325.5(7)	$9/2^-$	$7/2^-$
50.0(5)	55(18)	189(61)		M1	187.7(7)	137.8(7)	$3/2^-$	$1/2^-$
(53.1)(5)	3(1)	35(15)		M1	454.4(7)	401.3(7)	$(5/2^-)$	$(5/2^-)$
71.8(5)					209.6(7)	137.8(7)	$5/2^-$	$1/2^-$
74.8(5)	5.7(9)	33(5)		M1	476.1(7)	401.3(7)	$(7/2^-)$	$(5/2^-)$
75.8(5)	5(3)	26(15)		M1	401.3(7)	325.5(7)	$(5/2^-)$	$7/2^-$
85.3(5)	57(7)	238(29)		M1	85.3(5)	0.0	$9/2^+$	$7/2^+$
96.2(5)	5(2)	16(7)		M1	572.2(7)	476.1(7)	$(9/2^-)$	$(7/2^-)$
104.5(5)	9(2)	26(6)		M1	189.8(7)	85.3(5)	$11/2^+$	$9/2^+$
115.9(5)	24(2)	56(4)		M1	325.5(7)	209.6(7)	$7/2^-$	$5/2^-$
(130.4)(5)	5(1)	10(2)		M1	531.7(7)	401.3(7)	$(7/2^-)$	$(5/2^-)$
137.8(5)	24(2)	205(15)		E3	137.8(7)	0.0	$1/2^-$	$7/2^+$
137.8(5)	40(5)	72(9)		E2	325.5(7)	187.7(7)	$7/2^-$	$3/2^-$
154.8(5)	25(2)	38(3)		E2	364.4(7)	209.6(7)	$9/2^-$	$5/2^-$
170.9(5)	2.6(9)	4(1)		E2	572.2(7)	401.3(7)	$(9/2^-)$	$(5/2^-)$
191.7(5)	90(6)	118(9)		M1	401.3(7)	209.6(7)	$(5/2^-)$	$5/2^-$
213.6(5)	62(16)	77(20)		M1	401.3(7)	187.7(7)	$(5/2^-)$	$3/2^-$

^{163}Gd, the relative intensities referenced to the 454.4 keV transition with uncertainties of the last digit indicated in parenthesis, the internal conversion corrected intensities and the multipolarities assumed for these corrections, the energy of the initial and final levels as well as the spins of the initial and final levels for those levels with spin assignments.

IV. DISCUSSION

The level schemes in Figures 1 and 2 have been assembled based upon observed coincidences, intensity, and assigned level spacings. Choice of the ground state was informed by the structure of ^{165}Dy [4, 5] and confirmed by subsequent identification of transitions to the ground state. All spin assignments have been based upon systematics with ^{165}Dy [4, 5] and are supported by theoretical calculations discussed bellow.

The previously observed 85.3, 137.8 and (401.3) keV transitions and the newly observed 454.4, (476.1), 1037.4, (2374.9), 2396.2 keV transitions have been placed as populating the ground state which has been assigned a spin value of $7/2^+$. This assignment of $7/2^+$ as the ground state of ^{163}Gd is based upon systematics with ^{165}Dy [3–5]. Assignment of the $1/2^-$ band in ^{163}Gd was based upon systematics of the $1/2^-$ band structure observed in ^{165}Dy. A very similar structure is observed for the $1/2^-$ band in ^{165}Dy and in ^{163}Gd. In ^{165}Dy the following transitions are observed within the first $1/2^-$ band: 50.4, 72.8, 116.8, 139.1, and 156.2 for which the analogs in the proposed $1/2^-$ band in ^{163}Gd are 50.0, 71.8, 115.9, 137.8, and 154.8 keV. These transitions have been listed according to the levels between which they are observed in ^{165}Dy and the matching spin levels where they are proposed to be transitions in ^{163}Gd. Additional lower energy transitions within the first $1/2^-$ band of ^{165}Dy were observed at the energies of 22.4 and 39.5 keV, and according to the proposed scheme, would be expected within ^{163}Gd to be 21.8 and 38.9 keV. However, these transitions are in an energy region for which the internal conversion is very strong, there is significant contamination from x-rays, and the efficency of the Clover detectors is dropping rapidly in the region of the 21.8 keV transition. Thus, there not being direct observation of the 21.8 keV transition within the scope of this study is not disconcerting and has been included tentatively in the proposed level scheme based upon observations of subsequent transitions in gates which would otherwise not be coincident.

The 137.8 keV transition to ground has no clear direct observation in this work due to the presence of a transition of degenerate energy 137.8 keV. However, this transition exhibits enhancement of intensity in the singles spectrum consistent with the previously observed isomeric transition of 137.8 keV by Hayashi *et al.* [1]. With the observed peak intensity enhancement and the matching spacing of the associated single particle state, the $1/2^-$ band head is assigned to have an excitation of 137.8 keV. If it is taken that both the 108.2 keV transition in ^{165}Dy and the 137.8 keV transition in ^{163}Gd are pure E3 transitions, the half-life of the 137.8 keV transition can be roughly estimated according to the reduced transition probabilities for E3 transitions by assuming

TABLE II. Transitions in ^{163}Gd continued.

E_γ keV	I_γ %	E_i	E_f	J_i^π	J_f^π
400.9(5)	6(3)	726.4(7)	325.5(7)	$(5/2^-)$	$7/2^-$
401.3(5)	22(11)	401.3(7)	0.0	$(5/2^-)$	$7/2^+$
440.8(5)	6(1)	630.6(7)	189.8(7)	$(9/2^-)$	$11/2^+$
441.3(5)	4(3)	805.6(7)	364.4(7)		$9/2^-$
446.4(5)	27(2)	531.7(7)	85.3(5)	$(7/2^-)$	$9/2^+$
454.4(5)	100(5)	454.4(7)	0.0	$(5/2^-)$	$7/2^+$
459.1(5)	7(2)	668.6(7)	209.6(7)	$(3/2^-)$	$5/2^-$
476.1(5)	3(1)	476.1(7)	0.0	$(7/2^-)$	$7/2^+$
476.5(5)	4(1)	840.8(7)	364.4(7)	$(9/2^+)$	$9/2^-$
480.6(5)	8(2)	806.2(7)	325.5(7)	$(7/2^-)$	$7/2^-$
480.9(5)	24(3)	668.6(7)	187.7(7)	$(3/2^-)$	$3/2^-$
486.9(5)	2.8(6)	572.2(7)	85.3(5)	$(9/2^-)$	$9/2^+$
516.8(5)	46(11)	726.4(7)	209.6(7)	$(5/2^-)$	$5/2^-$
530.9(5)	41(3)	668.6(7)	137.8(7)	$(3/2^-)$	$1/2^-$
538.7(5)	21(2)	726.4(7)	187.7(7)	$(5/2^-)$	$3/2^-$
544.7(5)	5(2)	909.0(7)	364.4(7)	$(9/2^-)$	$9/2^-$
550.6(5)	2.4(8)	1588.0(11)	1037.4(10)		
583.0(5)	6(1)	1037.4(10)	454.4(7)		$(5/2^-)$
583.5(5)	6(2)	909.0(7)	325.5(7)	$(9/2^-)$	$7/2^-$
596.6(5)	6(2)	806.2(7)	209.6(7)	$(7/2^-)$	$5/2^-$
599.3(5)	7(2)	924.8(7)	325.5(7)		$7/2^-$
607.7(5)	9(2)	693.0(7)	85.3(5)	$(5/2^+)$	$9/2^+$
646.3(5)	22(2)	646.3(5)	0.0	$(3/2^+)$	$7/2^+$
651.0(5)	4(1)	840.8(7)	189.8(7)	$(9/2^+)$	$11/2^+$
671.7(5)	8(2)	757.0(7)	85.3(5)	$(7/2^+)$	$9/2^+$
693.0(5)	0(0)	693.0(7)	0.0	$(5/2^+)$	$7/2^+$
755.5(5)	3(1)	840.8(7)	85.3(5)	$(9/2^+)$	$9/2^+$
757.0(5)	4.6(5)	757.0(7)	0.0	$(7/2^+)$	$7/2^+$
786.8(5)	0(0)	2265.0(11)	1478.2(11)		
952.1(5)	3(1)	1037.4(10)	85.3(5)		$9/2^+$
974.8(5)	11(1)	1339.2(7)	364.4(7)		$9/2^-$
981.2(5)	9(2)	1306.7(7)	325.5(7)		$7/2^-$
992.4(5)	6.5(8)	1638.7(7)	646.3(7)		$(3/2^+)$
1002.1(10)	17(3)	1456.5(11)	454.4(7)		$(5/2^-)$
1015.1(10)	14(3)	1100.4(11)	85.3(5)		$9/2^+$
1037.4(10)	72(5)	1037.4(10)	0.0		$7/2^+$
1113.8(10)	4(1)	1478.2(11)	364.4(7)		$9/2^-$
1225.3(10)	4.3(7)	2262.7(14)	1037.4(10)		
1268.6(10)	0(0)	1478.2(11)	209.6(7)		$5/2^-$
1358.8(10)	5(2)	2396.2(14)	1037.4(10)		
1402.3(10)	9(1)	2439.7(14)	1037.4(10)		
1427.5(10)	7(1)	2527.9(14)	1100.4(11)		
1447.2(10)	21(4)	2484.6(14)	1037.4(10)		
1490.5(10)	1.1(4)	2527.9(14)	1037.4(10)		
1555.4(10)	0(0)	2396.2(14)	840.8(7)		$(9/2^+)$
1616.5(10)	3.6(9)	2262.7(14)	646.3(7)		$(3/2^+)$
1664.9(10)	4(1)	2311.1(11)	646.3(7)		$(3/2^+)$
1682.0(10)	0(0)	2374.9(11)	693.0(7)		$(5/2^+)$
1699.6(10)	10(2)	2154.0(11)	454.4(7)		$(5/2^-)$
1713.2(10)	14(1)	2439.6(14)	726.4(7)		$(5/2^-)$
1717.7(10)	0(0)	2410.6(11)	693.0(7)		$(5/2^+)$
1721.6(10)	4(3)	2527.8(14)	806.2(7)		$(7/2^+)$

TABLE III. Transitions in ^{163}Gd continued.

E_γ keV	I_γ %	E_i	E_f	J_i^π	J_f^π
1721.7(10)	5.2(6)	2253.5(11)	531.7(7)		(7/2-)
1728.7(10)	6(1)	2374.9(11)	646.3(7)		(3/2+)
1738.9(10)	2(1)	2311.1(11)	572.2(7)		(9/2-)
1750.0(10)	1.3(6)	2396.2(14)	646.3(7)		(3/2+)
1758.2(10)	21(2)	2484.6(14)	726.4(7)		(5/2-)
1764.4(10)	1.3(6)	2410.6(11)	646.3(7)		(3/2+)
1771.0(10)	25(2)	2439.6(14)	668.6(7)		(3/2-)
1799.1(10)	0.8(8)	2253.5(11)	454.4(7)		(5/2-)
1801.4(10)	4.5(7)	2527.8(14)	726.4(7)		(5/2-)
1808.3(10)	3(2)	2262.7(14)	454.4(7)		(5/2-)
1816.0(10)	30(2)	2484.6(14)	668.6(7)		(3/2-)
1834.7(10)	8(4)	2236.0(11)	401.3(7)		(5/2-)
1838.4(10)	4(1)	2484.6(14)	646.3(7)		(3/2+)
1856.7(10)	7(2)	2311.1(11)	454.4(7)		(5/2-)
1859.1(10)	3(1)	2527.8(14)	668.6(7)		(3/2-)
1903.6(10)	4(2)	2358.0(11)	454.4(7)		(5/2-)
1909.8(10)	3(1)	2311.1(11)	401.3(7)		(5/2-)
1956.7(10)	5(2)	2320.5(11)	364.4(7)		9/2-
1985.2(10)	1.8(6)	2439.6(14)	454.4(7)		(5/2-)
1996.1(10)	4(7)	2527.8(14)	531.7(7)		(7/2-)
2030.2(10)	17(2)	2484.6(14)	454.4(7)		(5/2-)
2126.5(10)	5.7(7)	2527.8(14)	401.3(7)		(5/2-)
2165.9(10)	9(5)	2491.4(11)	325.5(7)		7/2-
2177.4(10)	27(4)	2262.7(14)	85.3(5)		9/2+
2202.3(10)	38(3)	2527.8(14)	325.5(7)		7/2-
2217.4(10)	5(1)	2542.9(11)	325.5(7)		7/2-
2221.4(10)	8(2)	2585.8(11)	364.4(7)		9/2-
2235.2(10)	24(4)	2320.5(11)	85.3(5)		9/2+
2247.0(10)	3(1)	2332.3(11)	85.3(5)		9/2+
2260.2(10)	2(2)	2585.8(11)	325.5(7)		7/2-
2275.0(10)	67(5)	2484.6(14)	209.6(7)		5/2-
2296.9(10)	32(3)	2484.6(14)	187.7(7)		3/2-
2310.9(10)	54(6)	2396.2(14)	85.3(5)		9/2+
2317.6(10)	3(1)	2402.9(11)	85.3(5)		9/2+
2325.3(10)	7(2)	2410.6(11)	85.3(5)		9/2+
2346.8(10)	8(1)	2484.6(14)	137.8(5)		1/2-
2374.9(10)	29(2)	2374.9(11)	0.0		7/2+
2396.2(10)	5.3(8)	2396.2(14)	0.0		7/2+
2431.0(10)	3(3)	2516.3(11)	85.3(5)		9/2+
2490.1(10)	2.3(7)	2575.4(11)	85.3(5)		9/2+
2576.4(10)	3(1)	2661.7(11)	85.3(5)		9/2+

the same reduced transition probability for both transitions. As the half-life of the 108.2 keV transition was observed to be 1.257 minutes [10], the half-life of the 137.8 keV transition would be estimated as 13.9s. This is according to the energy relationship for reduced transition probabilities as discussed in Alder and Steffen's text [11]. Hayashi *et al.*'s observation of a 23.5(10)s half-life is then consistent with an E3 transition [1]. As there is only a single γ transition following the proposed isomer,

TABLE IV. Internal Conversion Corrected γ Feeding and γ Outflow in ^{163}Gd. J^π assignments in the current work from systematics with ^{165}Dy, [3–5].‡ Expected isomeric state. †Neither the expected 21.8 keV transition from 209.6 keV level to 187.7 keV level nor the 71.8 keV transition to the 137.8 keV level could be fit for relative intensity assignment.

E_{Level} keV	γ Feeding	γ Outflow	J^π	E_{Level} keV	γ Feeding	γ Outflow	J^π
0.0	702(36)	0(0)	7/2+	1339.2(7)	0(0)	11(1)	
85.3(5)	219(12)	238(29)	9/2+	1456.5(11)	0(0)	17(3)	
137.8(7)‡	237(61)	205(15)	1/2-	1478.2(11)	0(0)	4(1)	
187.7(7)	226(22)	189(61)	3/2-	1588.0(11)	0(0)	2.4(8)	
189.8(7)	10(2)	26(6)	11/2+	1638.7(7)	0(0)	6.5(8)	
209.6(7)†	337(16)		5/2-	2154.0(11)	0(0)	10(2)	
325.5(7)	141(21)	127(10)	7/2-	2236.0(11)	0(0)	8(4)	
364.4(7)	42(5)	62(13)	9/2-	2253.5(11)	0(0)	6(1)	
401.3(7)	99(16)	244(29)	(5/2-)	2262.7(14)	0(0)	38(4)	
454.4(7)	67(5)	135(16)	(5/2-)	2265.0(11)	0(0)	0(0)	
476.1(7)	16(7)	36(5)	(7/2-)	2311.1(11)	0(0)	17(3)	
531.7(7)	9.3(9)	38(3)	(7/2-)	2320.5(11)	0(0)	29(5)	
572.2(7)	2(1)	23(7)	(9/2-)	2332.3(11)	0(0)	3(1)	
630.6(7)	0(0)	6(1)	(9/2-)	2358.0(11)	0(0)	4(2)	
646.3(5)	26(2)	22(2)	(3/2+)	2374.9(11)	0(0)	35(3)	
668.6(7)	58(3)	71(5)	(3/2-)	2396.2(14)	0(0)	65(6)	
693.0(7)	0(0)	9(2)	(5/2+)	2402.9(11)	0(0)	3(1)	
726.4(7)	39(2)	74(12)	(5/2-)	2410.6(11)	0(0)	8(2)	
757.0(7)	0(0)	12(2)	(7/2+)	2439.6(14)	0(0)	50(3)	
805.6(7)	0(0)	4(3)		2484.6(14)	0(0)	200(8)	
806.2(7)	4(3)	14(3)	(7/2-)	2491.4(11)	0(0)	9(5)	
840.8(7)	0(0)	12(2)	(9/2+)	2516.3(11)	0(0)	3(3)	
909.0(7)	0(0)	11(3)	(9/2-)	2527.8(14)	0(0)	69(5)	
924.8(7)	0(0)	7(2)		2542.9(11)	0(0)	5(1)	
1037.4(10)	43(4)	81(6)		2575.4(11)	0(0)	2.3(7)	
1100.4(11)	7(1)	14(3)		2585.8(11)	0(0)	10(3)	
1306.7(7)	0(0)	9(2)		2661.7(11)	0(0)	3(1)	

a half-life on the order of seconds would prevent the experimental setup from observing any coincident γ-rays or β-rays. This would result in enhancement of the transition in the singles spectrum without any further evidence and an observed excess of γ feeding compared to γ outflow for the associated level. which is consistent with our observations. Furthermore the assignment of $1/2^-$ being above the $7/2^+$ state is consistent with studies by Hartley, *et al.* [6]. Wherein the ordering of the $\nu 7/2[633]$, $\nu 1/2[521]$, and $\nu 5/2[523]$ single particle states is well discussed for the nearby N=98 ^{162}Gd.

Assignment of the $3/2^-$ band comes from the six strongest transitions observed exiting the band in Figure 3 frames (d) and (f). The gate on 1758.2 keV shown in frame (f) shows the 400.9, 516.8, and 538.7 keV transitions which correspond to the three transitions from the 726.4 keV $(5/2^-)$ level to the 325.5 keV $7/2^-$, 209.6 keV $5/2^-$, and 187.7 keV $3/2^-$ levels, respectively. Similarly, frame (d) shows coincident spectra for the gate on the 1816.0 keV transition. Therein peaks of 459.1, 480.9, and 530.9 keV correspond to the three transitions from the 668.6 keV level to the 209.6 keV $5/2^-$, 187.7 keV $3/2^-$, and 137.8 keV $1/2^-$ levels, respectively. For both of these coincidence spectra, it is clearly seen that only three transitions are well observed exiting the $3/2^-$ band at each of these levels. Although allowed from a $5/2^-$ level, no transition has been observed to the $7/2^+$ ground state band from these levels. Similar transitions between the $3/2^-$ band and the $1/2^-$ band in ^{165}Dy are observed. Thus, the 668.6, 726.4, 806.2, and 909.0 keV levels have been tentatively assigned to the $(3/2^-)$ band in ^{163}Gd.

The 454.4 keV level is low enough in energy for anticipated single particle states and has been tentatively assigned as the $5/2^-[512]$ band head along with the 531.7, and 630.6 keV levels as the $(7/2^-)$, and $(9/2^-)$ rotational excitations respectively. The resultant level spacing is consistent with the PSM calculations. It is possible that the 454.4 keV is associated with the $7/2^-[514]$ neutron level resulting in an incease of one spin for all these assingments, both would be consistent with the strong apparent β-feeding received by the 454.4 keV level given a $(5/2^-)$ parent ground state.

Evidence for the 170.9 keV transition is weak com-

pared to the other proposed transitions. However, the 170.9 and 74.8 keV transitions would be consistent with the structure of the $5/2^-$ band observed in ^{165}Dy and a 486.9 keV transition has been observed that would be consistent with the placement of a 572.2 keV $9/2^-$ level. The competition between the 486.9 keV transition and the 170.9 keV transition would explain the reduced intensity observed for the 170.9 keV transition. Thus the 170.9 keV transition is not listed as tentative.

The 646.3 keV level observes γ-feeding from a number of levels around 2 MeV. Review of the observed γ-feeding compaired to outflow shows that this level is expected to have no β-feeding. As a result, the 646.3 keV level has been tentatively assigned as the band head of the 3/2+ band and several similarly low β-fed levels have tentatively been assigned as the rotational excitations at levels 693.0 (5/2+), 757.0 (7/2+), and 840.8 (9/2+) keV.

Table IV lists the internal conversion corrected feeding and outflow observed from γ relative intensity measurements for ^{163}Gd. A review of Table IV shows feeding and outflow relationships consistent with very limited β-feedings for both the 85.3 and 189.8 keV levels in the 7/2+ groundstate band. The ground state of the parent nucleus is tentatively expected to have a spin of $5/2^+$ based upon the tentative ground state deformation of the two proton analog of ^{163}Eu, ^{165}Tb. Such a low spin for the ground state of the parent is consistent with the low apparent β-feeding of the groundstate band as even the lowest level at 85.3 keV has a spin of 9/2+ which would be at least a first forbidden transition. If the parent isotope does indeed have a ground state spin of $5/2^+$, population of the $3/2^+$ should be preferred to all of the observed bands. A lack of a well populated $3/2^+$ but strongly populated $1/2^-$, $3/2^-$, and $5/2^-$ bands, offers support of the parent ground state being not $5/2^+$ with deformation similar to the +2 proton neutron analog but $5/2^-$. With a parent ground state of $5/2^-$, the weak population of the even parity bands is reconciled.

Another feature of note observed on Table IV is for the 209.6 keV level which exhibits an excess of observed γ feeding relative to the observed γ outflow. This is due to the previously discussed unobserved 21.8 keV transition to the 187.7 keV level expected from systematics with ^{165}Dy. This transition is likely present and very strongly internaly converted. The existance of this transition would not only help explain the lack of observed transitions from the 209.6 keV level but also the discrepancy between γ-feeding and outflow of the 187.7 keV level that otherwise could only be explained by strong direct population of the 187.7 keV level following β-decay. Furthermore the 71.8 keV transition was not fit without significant contamination from either background sources or coincident transitions of similar energy, as a result the γ-outflow from this level was not ascertained.

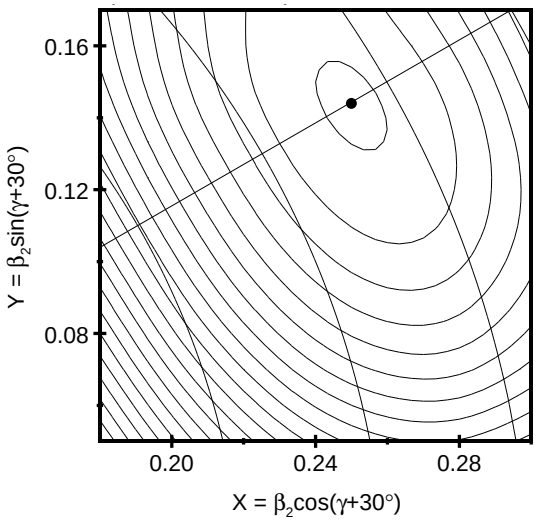

FIG. 4. PES calculation for $\nu 1/2^-[521]$. β_2=0.286, γ=0, β_4=0.028.

IV.1. Potential Energy Surface Calculations

The configuration-constrained potential-energy surface (PES) method [12] is employed with a nonaxial deformed Woods-Saxon potential [13] with universal parameters to generate single-particle levels. The Lipkin-Nogami method [14] is employed to avoid the spurious transition encountered in the BCS approach. The total energy of a nucleus can be decomposed into a macroscopic part obtained from the standard liquid-drop model and a microscopic part computed with the shell-correction approach including blocking effects. The deformation, excitation energy, and pairing property of a given state are determined by minimizing the obtained PES.

PES calculations were performed for the following configurations: $\nu 1/2^-[521]$, $\nu 7/2^+[633]$, $\nu 5/2^-[523]$, $\nu 5/2^+[642]$, and $\nu 5/2^-[512]$. The deformations yielded by these calculations were consistent with a deformed nucleous without any expected shape coexistance. Figure 4 is the plot of the $\nu 1/2^-[521]$ PES calculation.

IV.2. Projected Shell Model Calculation

The active nucleon configurations that can be assigned to the bands observed in ^{163}Gd have been calculated using the projected shell model (PSM) [15, 16] and those calculated energy levels and comparison with the experimental data are given in Figure 5. PSM has been successfully applied for studying the structure of isomer states for $A \sim 100, 160$ and 180 neutron-rich mass region [17–19].

In the present calculations, we use $\varepsilon_2 = 0.275$, $\varepsilon_4 = 0.000$, a value which is indicated by total Routhian surface calculations [20]. The monopole-pairing strength is taken to be $G_M = [G_1 \mp G_2(N-Z)/A]/A$, "-" for neutrons and "+" for protons, with $G_1 = 20.12$ and $G_2 =$

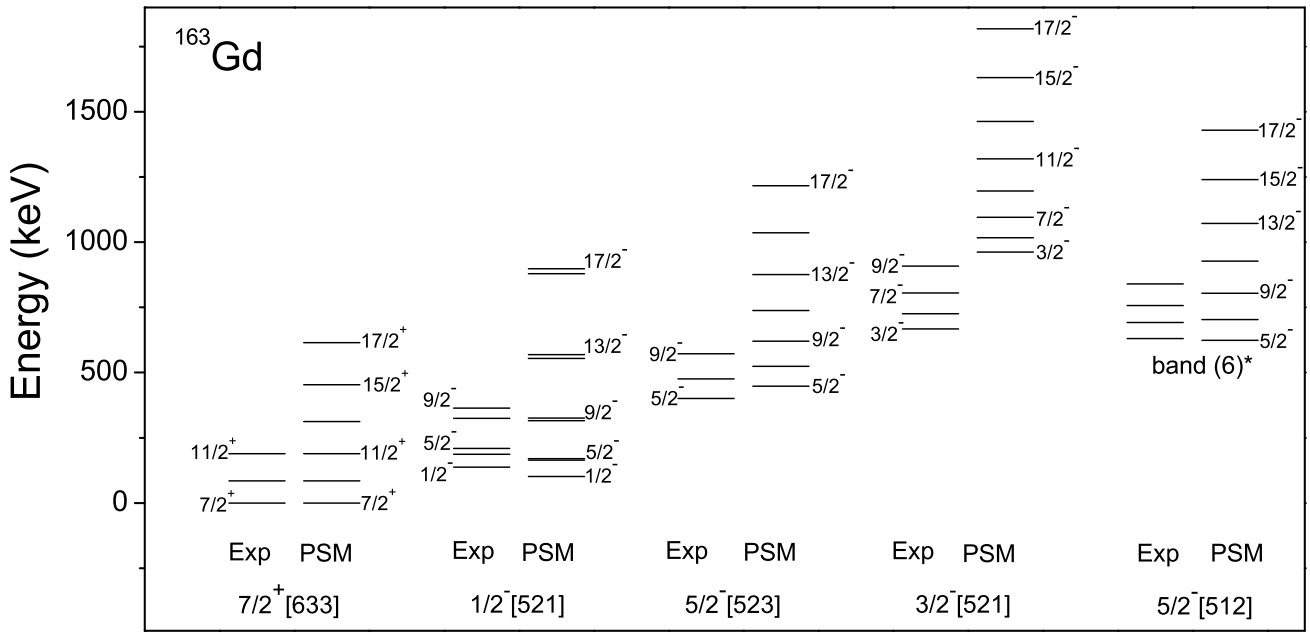

FIG. 5. Comparison of proposed bands of ^{163}Gd with calculated band structure of ^{163}Gd.

13.13 being the coupling constants. The quadrupole-pairing strength G_Q is assumed to be proportional to G_M, with the proportionality constant being fixed to be 0.16. These strengths are consistent with those used in previous works for the same mass region [18].

In Figure 5, rotational bands up to 17/2 of spin are plotted. The dominant configuration for each rotational band is labeled and discussed in the following part below. The calculated $7/2^+[633]$ ground state is in good agreement with the experimental data together with the $N = 99$ systematics [21]. The first excited state is assigned as $1/2^-[521]$ in the PSM calculations, which is in good agreement with the experimental data. The correct placement of the $7/2^+[633]$ and $1/2^-[521]$ neutron single particle orbital are most important to understand the evidence of the $N = 98$ subshell gap [6]. With the neutron Fermi surface moving up, the $5/2^-[523]$ one-quasiparticle (1-qp) state is more excited which is the ground state for the $N = 97$ isotones in $A \sim 160$ mass region. Both the energy levels and the dominant configuration for these three bands are reproduced well by the PSM calculations. However, the calculated energy levels of the $3/2^-[521]$ 1-qp band are higher than those of experimental data. In Reference [22, 23], β_6 or ε_6 deformation was included in the potential energy surface calculations and cranked shell model, respectively, which is not taken into account in the present calculations. It is expected that theoretical results will be improved with including high order deformation. For band (6)*, no spin and parity assignment are obtained experimentally. In our PSM calculation, a 1-qp band with $5/2^-[512]$ configuration is predicted with the band head energy of 624.2 keV, which is in good agreement with the experimental excitation energy of 630.6 keV. The predicted energy levels of high spin states in Figure 5 may provide a guidance to the further experimental work.

V. CONCLUSION

The structure of ^{163}Gd has been identified for the first time and compared with the structure of ^{165}Dy, the neutron analog of ^{163}Gd. Assignments of the ground state band and five additional bands have been proposed. The ground state has been asigned a spin of $7/2^+$, comenserate with the ground state of the +2 proton neutron-analog ^{165}Dy. The initial observations of the 137.8 keV level by Hayashi *et al.* [1] as isomeric has been confirmed with the level being observed as the first excited state at 137.8 keV and a spin of $1/2^-$. This assignment is both consistent with the structure of ^{165}Dy and the observation of the level as an isomer. Two bands of spin $5/2^-$ are tentatively porposed at 401.3 and 454.4 keV. The 668.6 keV level is tentatively proposed to be the band head of the $3/2^-$ band. Lastly a band head of $3/2^+$ is tentatively proposed at 646.3 keV.

A single parameter was implemented in PSM calculations. This is consistent with the PES calculation as it did not yield any expectation of shape coexistance. PSM calculations yielded good agreement with experimentally

observed band structures in four out of five cases. For the remaining case of the $3/2^-$ band it is expected that higher order deformation would need to be included in the calculation to resolve this discrepancy.

This structure represents the authors best observable structure from the setup of this experiment. Further structure beyond level spacing and observed γ intinsities for ^{163}Gd would need to be performed with a setup capable of more complete efficiency, including absolute count of β-decay events and, or, increased angular resolution such that angular correlation measurements could be implemented to make confident spin asignments.

VI. ACKNOWLEDGEMENTS

Work at Oak Ridge National Laboratory and Vanderbilt University was supported by Department of Energy grant number: DE-FG05-88ER-40407. Support for the work done at Huzhou University was provided by the National Natural Science Foundation of China grant numbers: U1832139, 11847315, 11575112, and 11747312, and by the National Key Program for S&T Research and Development grant number: 2016YFA0400501. Work at Peking University was supported by the National Natural Science Foundation of China grant numbers: 11835001, and 111575007.

[1] H. Hayashi, M. Shibata, M. Asai, A. Osa, T. Sato, M. Koizumi, A. Kimura, and M. Oshima, Nucl. Instrum. Methods Phys. Res. Sect. A **747**, 41 (2014).
[2] T. K. Sato, A. Osa, K. Tsukada, M. Asai, H. Hayashi, Y. Kojima, M. Shibata, and S. Ichikawa., JAEA-Review 2006-029 , 31 (2006).
[3] R. K. Sheline, W. N. Shelton, H. T. Motz, and R. E. Carter, Phys. Rev. **136**, B351 (1964).
[4] R. C. Greenwood, R. J. Gehrke, J. D. Baker, D. H. Meikrantz, and C. W. Reich, Phys. Rev. C **27**, 1266 (1983).
[5] E. Kaerts, P. H. M. van Assche, S. A. Kerr, F. Hoyler, H. G. Börner, R. F. Casten, and D. D. Warner, Nuclear Physics A **514**, 173 (1990).
[6] D. J. Hartley, F. G. Kondev, R. Orford, J. A. Clark, G. Savard, A. D. Ayangeakaa, S. Bottoni, F. Buchinger, M. T. Burkey, M. P. Carpenter, P. Copp, D. A. Gorelov, K. Hicks, C. R. Hoffman, C. Hu, R. V. F. Janssens, J. W. Klimes, T. Lauritsen, J. Sethi, D. Seweryniak, K. S. Sharma, H. Zhang, S. Zhu, and Y. Zhu, Phys. Rev. Lett. **120**, 182502 (2018).
[7] A. Osa, S. ichi Ichikawa, M. Matsuda, T. K. Sato, and S.-C. Jeong, Nucl. Instrum. Methods Phys. Res. Sect. B **266**, 4394 (2008).
[8] J. D. B. R. J. Gehrke, R. C. Greenwood and D. H. Mekrantz, Journal of Radioanalytical and Nuclear Chemistry **74**, 117 (1982).
[9] R. Grzywacz, Nucl. Instrum. Methods Phys. Res. Sect. B **204**, 649 (2003).
[10] H. Nabielek, *Untersuchung von Obergangsraten Elektromagnetischer Ubergange durch Messung der Lebensdauer Angeregter Kernniveaus nach Neutroneneinfang* (Physikinstitut, Reaktorzentrum Seibersdorf, Austria; SGAE-PH-78/1968, 1968).
[11] K. Alder and R. M. Steffen, in *The electromagnetic interaction in nuclear spectroscopy* (1975).
[12] F. Xu, P. Walker, J. Sheikh, and R. Wyss, Physics Letters B **435**, 257 (1998).
[13] W. Nazarewicz, J. Dudek, R. Bengtsson, T. Bengtsson, and I. Ragnarsson, Nuclear Physics A **435**, 397 (1985).
[14] H. Pradhan, Y. Nogami, and J. Law, Nuclear Physics A **201**, 357 (1973).
[15] K. Hara and Y. Sun, Int. J. Mod. Phys. E **4**, 637 (1995).
[16] Y. Sun, Phys. Scr. **91**, 043005 (2016).
[17] Y.-X. Liu, Y. Sun, X.-H. Zhou, Y.-H. Zhang, S.-Y. Yu, Y.-C. Yang, and H. Jin, Nucl. Phys. A **858**, 11 (2011).
[18] Y. C. Yang, Y. Sun, S. J. Zhu, M. Guidry, and C. L. Wu, J. Phys. G: Nucl. Part. Phys **37**, 085110 (2010).
[19] X.-Y. Wu, S. K. Ghorui, L.-J. Wang, Y. Sun, M. Guidry, and P. M. Walker, Phys. Rev.C **95**, 064314 (2017).
[20] Möller, J. Nix, W. Myers, and W. Swiatecki, At. Data Nucl. Data Tables **59**, 185 (1995).
[21] Z. Patel, P. M. Walker, Z. Podolyák, P. H. Regan, T. A. Berry, P.-A. Söderström, H. Watanabe, E. Ideguchi, G. S. Simpson, S. Nishimura, Q. Wu, F. R. Xu, F. Browne, P. Doornenbal, G. Lorusso, S. Rice, L. Sinclair, T. Sumikama, J. Wu, Z. Y. Xu, N. Aoi, H. Baba, F. L. Bello Garrote, G. Benzoni, R. Daido, Z. Dombrádi, Y. Fang, N. Fukuda, G. Gey, S. Go, A. Gottardo, N. Inabe, T. Isobe, D. Kameda, K. Kobayashi, M. Kobayashi, T. Komatsubara, I. Kojouharov, T. Kubo, N. Kurz, I. Kuti, Z. Li, M. Matsushita, S. Michimasa, C.-B. Moon, H. Nishibata, I. Nishizuka, A. Odahara, E. Şahin, H. Sakurai, H. Schaffner, H. Suzuki, H. Takeda, M. Tanaka, J. Taprogge, Z. Vajta, A. Yagi, and R. Yokoyama, Phys. Rev.C **95**, 034305 (2017).
[22] Z. Patel, P.-A. Söderström, Z. Podolyák, P. H. Regan, P. M. Walker, H. Watanabe, E. Ideguchi, G. S. Simpson, H. L. Liu, S. Nishimura, Q. Wu, F. R. Xu, F. Browne, P. Doornenbal, G. Lorusso, S. Rice, L. Sinclair, T. Sumikama, J. Wu, Z. Y. Xu, N. Aoi, H. Baba, F. L. Bello Garrote, G. Benzoni, R. Daido, Y. Fang, N. Fukuda, G. Gey, S. Go, A. Gottardo, N. Inabe, T. Isobe, D. Kameda, K. Kobayashi, M. Kobayashi, T. Komatsubara, I. Kojouharov, T. Kubo, N. Kurz, I. Kuti, Z. Li, M. Matsushita, S. Michimasa, C.-B. Moon, H. Nishibata, I. Nishizuka, A. Odahara, E. Şahin, H. Sakurai, H. Schaffner, H. Suzuki, H. Takeda, M. Tanaka, J. Taprogge, Z. Vajta, A. Yagi, and R. Yokoyama, Phys. Rev. Lett. **113**, 262502 (2014).
[23] X.-T. He and Y.-C. Li, Phys. Rev.C **98**, 064314 (2018).